Hindawi
International Journal of Photoenergy
Volume 2022, Article ID 9353470, 12 pages
https://doi.org/10.1155/2022/9353470

*Research Article*

# Artificial Deep Neural Network in Hybrid PV System for Controlling the Power Management

**Satyajeet Sahoo**,[1] **T. M. Amirthalakshmi**,[2] **S. Ramesh**,[3] **G. Ramkumar**,[4] **Joshuva Arockia Dhanraj**,[5] **A. Ranjith**,[6] **Sami Al Obaid**,[7] **Saleh Alfarraj**,[8] **and S. S. Kumar**[9]

[1]*Department of Electronics and Communication Engineering, Vignan's Foundation for Science, Technology and Research (Deemed to Be University), Vadlamudi, Guntur, Andhra Pradesh 522213, India*
[2]*Department of Electronics and Communication Engineering, Vel Tech Multi Tech Dr. Rangarajan Dr. Sakunthala Engineering College, Avadi, Chennai-600062, Tamil Nadu, India*
[3]*Department of Electronics and Communication Engineering, St. Mother Theresa College of Engineering, Vagaikulam, 628102 Tamil Nadu, India*
[4]*Department of Electronics and Communication Engineering, Saveetha School of Engineering, SIMATS, Chennai, 602 105 Tamil Nadu, India*
[5]*Centre for Automation and Robotics (ANRO), Department of Mechanical Engineering, Hindustan Institute of Technology and Science, Padur, Chennai, 603103 Tamil Nadu, India*
[6]*Department of Electronics and Communication Engineering, St. Joseph University in Tanzania, Dar es Salaam, Tanzania*
[7]*Department of Botany and Microbiology, College of Science, King Saud University, P.O. Box 2455, Riyadh 11451, Saudi Arabia*
[8]*Zoology Department, College of Science, King Saud University, Riyadh 11451, Saudi Arabia*
[9]*Department of Bioenvironmental Energy, College of Natural Resources & Life Science, Pusan National University, Miryang-si 50463, Republic of Korea*

Correspondence should be addressed to G. Ramkumar; pgrvlsi@gmail.com and A. Ranjith; ranjith.arumugam@sjuit.ac.tz

Received 18 January 2022; Revised 29 January 2022; Accepted 5 February 2022; Published 10 March 2022

Academic Editor: V. Mohanavel



The analysis of different components of a grid-linked hybrid energy system (HES) comprising a photovoltaic (PV) system is presented in this work. Due to the increase of the population and industries, power consumption is increasing every day. Due to environmental issues, traditional power plants alone are insufficient to supply customer demand. In this case, the most important thing is to discover another approach to meet customer demands. Most wealthy countries are now concentrating their efforts on developing sustainable materials and investing considerable amounts of money in product development. Wind, solar, fuel cells, and hydro/water resources are among the most environmentally benign renewable sources. To control the variability of PV generation, this sort of application necessitates the usage of energy storage systems (ESSs). Lithium-ion (Li-ion) batteries are the most often used ESSs; however, they have a short lifespan due to the applied stress. Hybrid energy storage systems (HESSs) started to evolve as a way to decrease the pressure on Li-ion batteries and increase their lifetime. This study represents a great power management technique for a PV system with Li-ion batteries and supercapacitor (SC) HESS based on an artificial neural network. The effectiveness of the suggested power management technique is demonstrated and validated using a conventional PV system. Computational models with short-term and long-term durations were used to illustrate their effectiveness. The findings reveal that Li-ion battery dynamical stress and peak value are reduced, resulting in longer battery life.

## 1. Introduction

In today's world, energy is critical to industrialization, urbanization, and a country's economic progress. According to the US EIA report, worldwide energy consumption is increasing at a rate of about 2.3 percent each year. According to the analysis, gasoline will be in short supply around the planet soon. Energy sources are the primary source of pollutants in the environment, including air and water contamination. As a result, renewable energy (RE) resources such as groundwater, air, photovoltaic, biofuels, and others have gotten more attention as potential energy individual behavioral. Renewable technologies, according to Kumar's research, are ubiquitous and affordable and polluted air [1]. Hybrid power systems are used to deliver loads and ensure load demand without the need for human involvement. People can use a variety of sources, including conventional sources such as coal, natural gas, and fossil fuels, as well as renewable technologies such as solar, wind, and hydroelectric. In addition to energy, a hybrid system includes DC or AC converters, a storage capability, and a process control enabling energy monitoring. A fuel cell functions as a battery, storing energy in the form of hydrogen [2]. It produces water and electricity by reacting hydrogen with atmospheric oxygen. However, multiple energy sources are required, such as the use of batteries in a rechargeable battery to harvest oxygen from the water or air, which results in a greater hydrogen storage price.

The goal of optimization algorithm-based strategies is to minimize an optimal solution. In general, the goal of reduction of this objective function is to lower the operational cost over a given period or to extend the lifespan of the HESS pieces. There are two sorts of strategies in this classification: optimization algorithm strategies and real-time optimization techniques. Based on a past understanding of future operational conditions, optimization algorithm strategies are devised to produce the best global solution [3]. Because of the higher processing expenses, this theory's real-time use has been restricted; this is generally only used to obtain a standard response to assess and change. Mathematical model, dynamic software, evolutionary algorithms, optimal controllers, and particle swarm optimization are some of the global optimization methodologies (PSO). Real-time optimization algorithms, on either extreme, use power supply choices to minimize an optimization problem. In particular, in both processing capacity and memory capacity, the mathematical modeling of this method must be appropriate for real-time implementation [4]. Pontryagin minimum principle (PMP), equivalent cost minimization strategy (ECMS), adaptive dynamic programming (ADP), model predictive control (MPC), extreme search (ES), artificial neural networks (ANNs), and robust control (RC) are all real-time optimizing methodologies.

An independent system with a HESS comprising Li-ion battery and SC, as well as a secondary storage resource, a fuel cell, was demonstrated with such a variable power control technique. Using a rolling average filter, the voltage regulation approach produces real-time values to the converters' speed controller connected with fuel cell, Li-ion batteries, and SC [5]. The simple moving machine's effectiveness is reinforced by simulation study experiments, which divide the average current reference between Li-ion batteries and fuel cells while efficiently distributing the rapid and oscillating demand elements to the SC. To manipulate the SOCs of the battery and the SCs and maintain it being within norms, an MPC voltage regulation approach was employed [6]. Given the complexity of using discrete modeling techniques and the high processing expense, this is a viable technique.

Photovoltaic technology is an excellent RES for controlling electromagnetic energy production from such a large centralized facility to a large number of tiny decentralized and distributed systems, reducing environmental impact and increasing resource production in remote places. The costs of photovoltaic components are rapidly decreasing, enabling photovoltaic systems more affordable than traditional energy sources [7]. Lithium battery packages and an energy storage stack make up the powerful engine of a typical proton electrolyte membrane hybrid hydrogen fuel cell. In this paper, a multiobjective optimum including fuel efficiency and system reliability is discussed for this commercial vehicle engine and transmission concept [8]. Given the complexity of using discrete modeling techniques and the high processing expense, this is a viable technique. A soft-run technique is given for the real-time and the interpredictive control method, based on the optimal results achieved by nonlinear optimization. The capacity of the lithium battery is taken into account to improve the soft-run method, which is carried out using two real-time algorithms. The energy requirement produces the best strategy which has proven to be the most suitable for power transit systems equipped with a bigger capacity battery, resulting in improved nonlinear programming results.

Classical control systems, such as RBC and frequency-based approaches, are still more susceptible to variable fluctuation and require an exact parametric representation, whereas optimization algorithm-based techniques are much more accurate and efficient [9]. As a result, artificial neural network-(ANN-) based optimization procedures are being designed to lessen the influence of parameter changes and to improve control methods. Due to its excellent generalization capabilities and nonlinear and adaptable architecture, which can improve the system dynamics without needing an accurate model, they can be successfully employed in process control.

An off-grid PV energy infrastructure with such a HESS comprised of a special type cell and lead-acid batteries was suggested using ANN-based power control. The proposed power requires managers to maintain a consistent battery SOC by controlling the electrolytes and hydrogen fuel outputs. In particular, compared to other approaches, simulated studies revealed that the suggested system has a fast response capability [10]. The high-frequency and low-frequency elements of a microgrid with such a HES made of Li-ion batteries and SC were separated using a wavelet treatment. To provide a better DC link voltage, a backpropagation ANN was also used to determine the current source of the Li-ion battery. The simulation experiments showed that the suggested power management can compensate for power variations from renewable electricity while keeping the DC voltage steady.

For powered mobility, an ANN-based power management technique was presented. A HES is used in the device, with Li-ion batteries permanently attached to the DC bus and SCs linked via a DC/DC conversion. The purpose of the installed ANN is to manage the SC DC/DC limit in addition to supporting Li-ion packs and increasing their lifetime. In comparison to battery-only ESSs, the simulations revealed a 64.8 percent increase in the lifetime of Li-ion batteries [11]. This presents a novel power strategic approach for HESSs based on ANN with low operating complexity, capable of managing the energy flow of all HESS components and extending the life of Li-ion battery systems by reducing dynamic strain and peak market requirements while consistently providing the stress only with demanded strength [12]. To maintain the protection and longevity of every ESS, the suggested energy management approach evaluates its SOC in real time and alters its charge/discharge commands. A typical standalone PV system with DC coupling and centralized control design was generated and constructed to test the effectiveness of the suggested battery management technique.

## 2. Related Works

A method for operating a grid-connected hybrid approach is presented in this study [13]. A control scheme with a photovoltaic (PV) array and a proton exchange membrane fuel cell (PEMFC) is being studied. When fluctuations in temperature and irradiance happen, the PV array usually employs a maximum power point tracking (MPPT) approach to continually send the greatest energy to the system, making it an uncontrolled source. The hybrid system's input voltage is controlled thanks to the PEMFC. Unit-power control (UPC) and feeder-flow control (FFC) are different operating methods that can be used with a hybrid system. The presentation covers the coordinating of two input modes, the synchronization of the PV system as well as the PEMFC within a hybrid power system, and also the derivation of estimate. The suggested operating strategy with variable operation mode shift always maintains the PV module at peak voltage and the PEMFC through its highly efficient performing band, resulting in improved performance and reliability, increased stability of the system, and fewer operating mode transitions.

A technology known as maximum power point tracking (MPPT) is used to improve photovoltaic (PV) power-generating efficiency. For quick climate changes and partial shade circumstances, this work offers a hybrid MPPT algorithm combining the modified invasive weed optimization (MIWO) and perturb and observe (P&O) techniques for effective removal of peak power from such a freestanding PV-based hybrid model. To obtain speedy global peak (GP) and maximal PV power, MIWO manages the earliest phases of MPPT and tests the effectiveness of the P&O algorithm in the latter stages. The PV system, batteries, accumulator, hydrogen fuel, and demand are all part of the microgrid under investigation. To protect the batteries from unwanted charging/discharging operations, a synchronized DC voltage-regulating and voltage control technique is

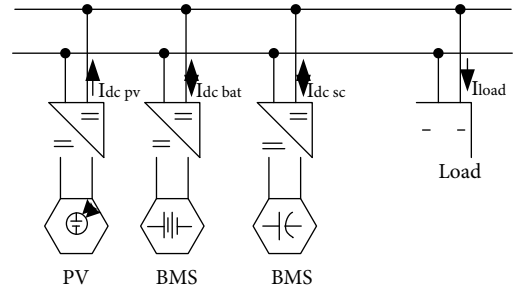


Figure 1: Implemented system block diagram.

established between every component of the hybrid power system. Furthermore, with the measurement of DC voltage, the DC/DC converter connected to the battery and DC link functions as an MPPT circuit for the PV, eliminating the need for an additional specialized circuit. The Takagi-Sugeno (TS) fuzzy controller is used to suppress/mitigate microgrid energy oscillations caused by changes in solar irradiation and power consumption. When compared to a few of the existing methodologies, the findings clearly show that the proposed approach outperforms them [14].

Solar energy creation is sporadic. A photovoltaic (PV) system's ability to produce power constantly and reliably to a fluctuating load is practically impossible. Paralleling a controlled source, such as a fuel cell, with PV could be a method for supplying electricity to changeable loads. A power management solution for the microgrid network is necessary to manage the power source between fuel cells and PVs. This work provides a remote monitoring system for such a grid-connected PV and solid oxide fuel cell (SOFC) that takes a load and direct solar variations into account. The suggested system's goal is to draw as little electricity from the grid as possible while operating the SOFC within a certain range. Because the PV is operating at maximum output, the power management requires using a proportional and integral (PI) system to control the power factor of the SOFC. The genetic algorithm (GA) and simplex approach are used to estimate the parameter settings of a PI controller $K_p$ (proportional constants) and $T_i$ (essential time continual). In addition, to produce suitable control variables for the PI controller, a fuzzy controller is constructed. The sum of the advanced process by standard deviation (ITAE) criteria is used to measure the controls' effectiveness. The fuzzy-based PI controller beats the PI controller adjusted by GA and linear approach in regulating the energy first from mixed source efficiently under demand and solar irradiance fluctuations, according to numerical simulations [15].

Today, consumption is growing at a rapid rate, highlighting the need for renewable resources. Among the several sources of renewable energy, power through solar cells is found to be an excellent source. However, one disadvantage of renewable radiation is that it was not available at that time, necessitating the use of additional sources in conjunction with solar fuel to produce the process more accurately and effectively. So, when power generated from the sun is insufficient to fulfill the necessary load, a solar energy system is integrated with a diesel power system developed to supply

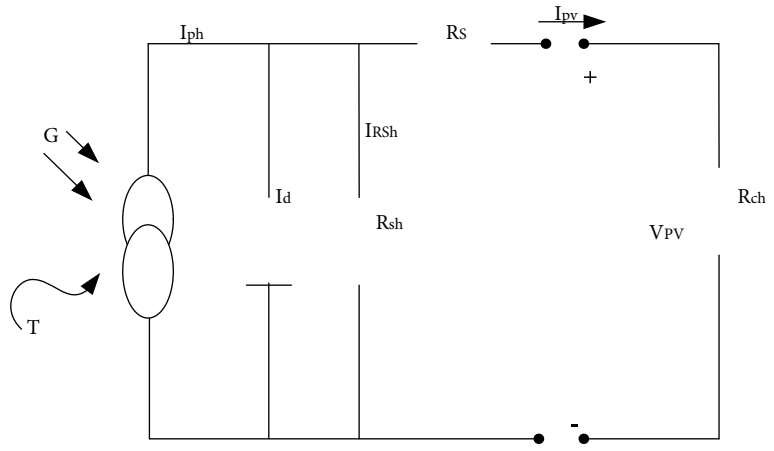


Figure 2: Boost converter.

the required. The battery energy storage technology is used as a backup device in this case (BESS). The PV-battery diesel combo is exported to the electrical to reach the necessary power consumption [16].

This research offers an energy management system (EMS) centered on artificial neural networks (ANNs) for regulating power in AC–DC hybrid distribution channels. The suggested ANN-based EMS gathers information like distributed generation (DG) energy, power system, and status of charge to determine the best operating mode (SOC). Profile information also on power conversion quantity of ESS for different distribution system energy scenarios was generated for learning the ANN, and also, the ANNs were educated with such a failure rate of less than 10%. In a grid-connected hybrid manner, the suggested EMS uses an already taught ANN to operate every voltage regulator in the best mode of operation. A modest hybrid AD/DC microgrid was built for model validation of the recommended EMS, and calculations and tests were conducted for each operating condition [17].

## 3. Materials and Methods

The equivalent circuit of the developed system is shown in Figure 1: a freestanding photovoltaic system using DC couplings and a logically centralized structure, composed of a PV unit, Li-ion battery, and SC. A buck-boost converter connects the PV unit's configurable sources and solar photovoltaic profile virtualization software configuration to the DC bus. Using the maximum power point tracking (MPPT) method, the buck-boost converter extracts the output power of the PV unit [18]. Two converters, DC/DC buck-boost converters, provide electron flow between its ESSs as well as the DC link. The system's major objective is to collect the highest available generated by the PV module to a DC bus at every given time, as well as capacity to control the energy flow among all HESS components while meeting the demand at any given time.

A Texas Electronics (Dallas, TX, USA) microprocessor TMS320F28069 serves as the actual control unit. This 32-bit fixed-point microcontroller is competent in parallel computing and is employed in mathematical applications of increasing difficulty. It operates at 90 MHz and has 100 kb and 2 kb of RAM and ROM memory, correspondingly, as well as 256 kb of flash memory. It also has 16 pulse width modulation (PWM) channels and 16 ADC channels with 12-bit precision and obtained using difference of roughly 333 nanoseconds. It also supports 12C, CAN, and SPI connectivity. Li-ion batteries and SC make up the HESS. Each of these ESSs is made up of several 12 units.

*3.1. PV Energy System.* To examine the nonlinear properties of PV generators related to semiconductor technology, different mathematical methods have been constructed [19]. The following model was proposed for this research:

PV current:

$$I_{pv} = I_{ph} - I_d - I_{Rsh}. \tag{1}$$

Then, the equation of current is given by

$$I_{pv} = I_{sc}\left\{1 - Q_1\left[\exp\left(U_2, R_{mpu} - 1\right)\right]\right\}, \tag{2}$$

where $U_1$, $U_2$, and $r$ are the coefficients given by

$$\begin{aligned} U_1 &= 0.01175, \\ U_2 &= \frac{U_4}{V_{oc}\, r}, \\ U_2 &= \ln\left[\frac{I_{sc}(1+U_1) - I_{mpp}}{U_1 + I_{sc}}\right], \\ U_4 &= \ln\left[\frac{1+U_1}{U_1}\right], \\ r &= \frac{\ln\left[U_2/U_4\right]}{\ln\left[V_{mpp}/V_{oc}\right]}. \end{aligned} \tag{3}$$

For standard test conditions (STP) of GSTC = 1000 W/

Table 1: ESS charge or discharge.

| | Boost converter | | Buck converter | | Buck-boost converter | |
|---|---|---|---|---|---|---|
| | Charge | Discharge | Charge | Discharge | Charge | Discharge |
| 1 | 0 | Pulse widthmodulation | $\overline{\text{Pulse width modulation}}$ | 0 | 0 | Pulse width modulation |
| 2 | 1 | $\overline{\text{Pulse width modulation}}$ | Pulse width modulation | 1 | Pulse width modulation | 1 |
| 3 | $\overline{\text{Pulse width modulation}}$ | 1 | 1 | Pulse width modulation | 1 | Pulse width modulation |
| 4 | Pulse width modulation | 0 | 0 | $\overline{\text{Pulse width modulation}}$ | Pulse width modulation | 0 |

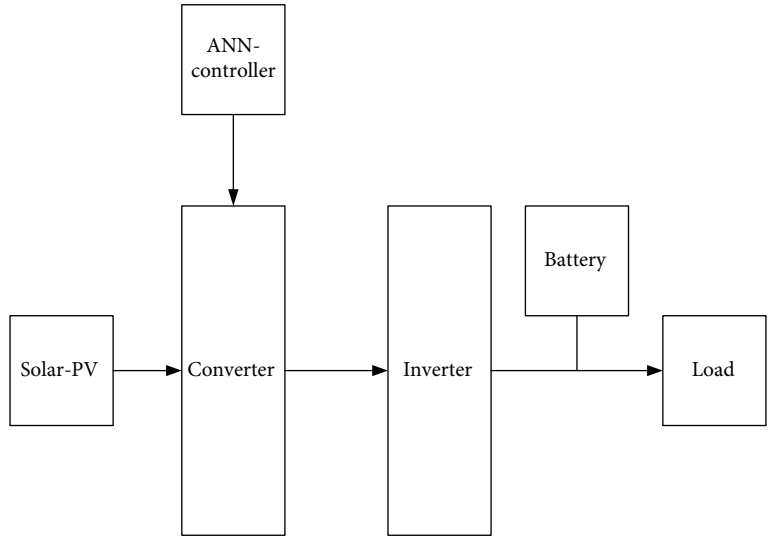


Figure 3: Configuration of the power management system.

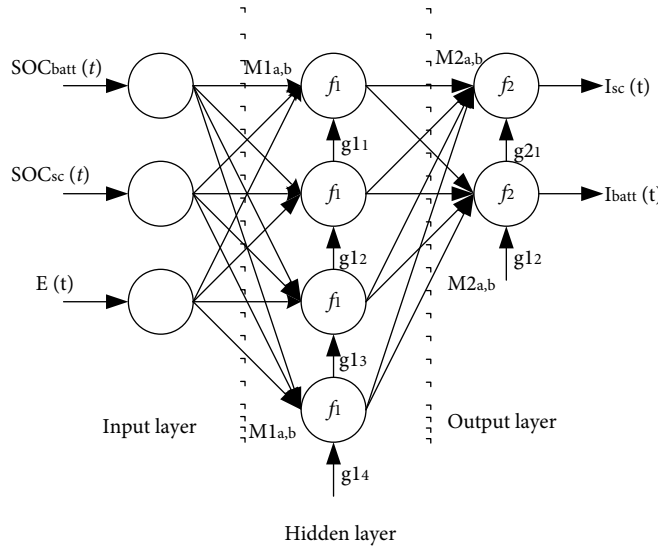


Figure 4: The architecture of a neural network.

$m^2$ and TSTC = 250 C, Equation (2) is only applicable for one irradiation level $G$ with module temperature $T_m$. According to the formulae, as temperatures and isolated change, other parameters change as well:

$$\Delta T_m = T_m - T_{STC},$$
$$\Delta I_{pv} = \alpha_{sc}\left(\frac{G}{G_{STC}}\right)\Delta T_m + \left(\frac{G}{G_{STC}} - 1\right) I_{sc,STC}. \quad (4)$$

Voltage of PV:

$$\Delta V_{pv} = -\beta_{oc}\Delta T_m - R_s \Delta I_{pv}. \quad (5)$$

*3.2. Boost Converter.* A boost converter in Figure 2 seems to be a DC to DC switching mode conversion with a higher output voltage than that of the input power. It was also known as a step-up converter. The inductance within the input signal resists abrupt fluctuations in input current, which boosts the converter's function [20]. It is stored in the inductor power in the induced electromagnetic force while switch $S$ is open and releases it because when switching $S$ is shut. The output circuit's capacitance is large enough because the outputs track's RC circuit's sampling frequency is high. When compared to the switching cycle, the sampling frequency is large, resulting in minimal output power.

$$V_o(t) = V_0(\text{constant}). \quad (6)$$

Duty cycle:

$$D = \frac{1 - V_{in(min)} \times \eta}{V_{out}}. \quad (7)$$

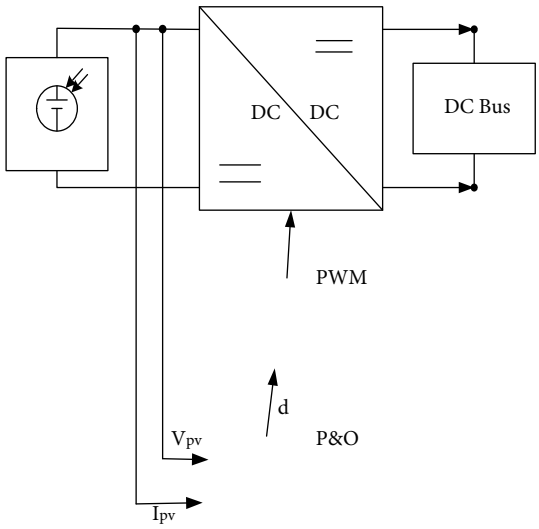


Figure 5: Control system of P&O.

Table 2: Parameter of PI controller.

| Controller | Parameter | Closed-loop current | Closed-loop voltage |
|---|---|---|---|
| $PI_{battery}$ | $K_i$ | 0.0043075 | 0.0207 |
| | $K_p$ | 1.7813 | 0.0515 |
| $PI_{SC}$ | $K_i$ | 0.0001 | 0.0001 |
| | $K_p$ | 0.7788 | 0.9378 |
| $PI_{reference}$ | $K_i$ | 0.005965 | 0.042 |
| | $K_p$ | 0.4 | 4.6145 |

Voltage output:

$$V_{\text{out}} = \frac{V_{\text{in}}}{1-D}, \qquad \Delta I_L = \frac{V_{\text{in(min)}} \times D}{f_s \times L}. \tag{8}$$

Current output:

$$I_{\text{max out}} = \left(I_{\text{lim(min)}} - \frac{\Delta I_L}{2}\right) \times (1-D). \tag{9}$$

*3.3. Inverter.* An inverter is a power electronic system that transforms DC electricity into AC power while also regulating the signal's amplitude, current, and speed. The DC power from a solar panel is sent to an inverter that transforms it to AC and delivers it to the demand in photovoltaic systems.

Voltage output:

$$V(t) = V_0 \cos(\omega t). \tag{10}$$

Current output:

$$I(t) = I_0 \cos(\omega t - \Psi). \tag{11}$$

Table 1 shows the difficult switching options for each ESS discharge and charge method of operation.

*3.4. Power Management System.* The benefits of the proposed PV hybrid power system using battery storage are dependent on several significant criteria, including the form and type of the load, speed, solar irradiation, cost of energy, and accessibility. For low-power applications, photovoltaic systems seem to be more cost-effective. The cost of electricity storage is an essential parameter to consider in the development of PV power systems using renewable power in automated vehicles [21]. To do so, one must analyze several different economic theories for each PV system separately. The fundamental rationale for PV systems would be to reduce the volume and cost of inventory. The suggested power generation system, as depicted in Figure 3, combines multiple sources of energy: PV as well as a battery as a backup. The ANN manager is in charge of managing natural resources. PV is considered a main/primary supplier by ANN-based power management controller (PMC) generator which is considered a supplementary source by ANN-based voltage regulation controller (PMC). The primary goal of a PMC for an autonomous combination is to meet load requirements in climatic variations while also managing power flow to ensure reliable functioning. Three control phases are recommended to complete the entire energy consumed by the load and recharge the batteries based on variations in irradiance, temperatures, and speed to determine the PV hybrid renewable energy system's capability.

The required control scheme and controlling techniques of a hybrid energy management system can vary considerably or even theoretically from those of conventional energy systems, depending on the classification and severity of available renewable energy component propagation, load behavior, and voltage stability restrictions. Because energy resource components, especially digitally coupled equipment, have distinct steady-state and dynamic properties than typical large turbine generating units [22], the intelligent control scheme for the proposed HES is depicted as a block diagram. For such specified solar irradiance and speed, a feed-forward ANN is used to calculate the operational maximum power point of hybrid power management. The training is performed using test data collected at various radiation levels.

As shown in Figure 4, the developed architecture employs a multilayer feed-forward neural network (FFNN). The information is transmitted without reflection in the interconnected neurons in this structure, i.e., the number of emissions does not quite have valuable feedback to all the other neural sources. Equations (12) and (13) can be used to depict the output layer which generates the reference signal ($I_{\text{ref bat}}$ and $I_{\text{ref SC}}$) in Figure 4:

$$I_{\text{ref bat}}(t) = f_2\left[\sum_b \left[\text{Rw}_{b,1} \times f_1\left[\sum_a Iw_{a,b} \times \begin{bmatrix} u_a \\ \text{SOC}_{\text{bat}}(t) \\ \text{SOC}_{\text{SC}}(t) \\ E(t) \end{bmatrix} + g_b\right]\right] + g_{2,1}\right], \tag{12}$$

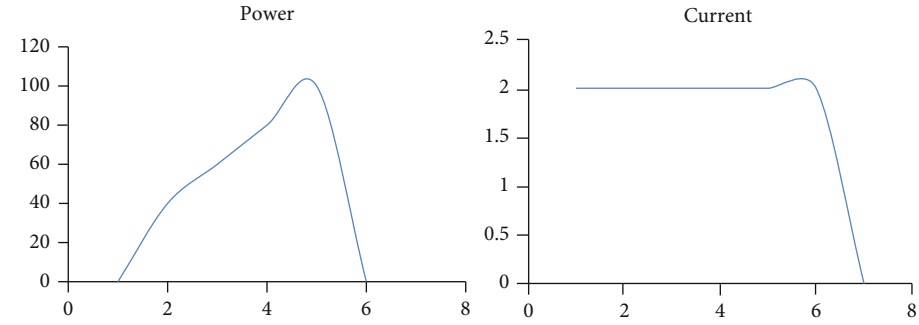


Figure 6: The curves of power voltage and the current voltage.

$$I_{\text{ref SC}}(t) = f_2\left[\sum_b \left[\text{Rw}_{b,2} \times f_1\left[\sum_a Iw_{a,b} \times \begin{bmatrix} \overset{u_a}{\widehat{\text{SOC}_{\text{bat}}}}(t) \\ \text{SOC}_{\text{SC}}(t) \\ E(t) \end{bmatrix} + g_b\right]\right] + g_{2,2}\right], \tag{13}$$

where $i$ is the number of iterations, $u_a$ is the data input matrix, $b$ is the number of hidden neurons, and $f_1$ and $f_2$ are the activation functions. The values of the connections between both the encoder and decoder layers are represented by Rw; the masses of the connections between both the hidden layer and output layer are represented by Lw, and the bias of a transistor in the corresponding layers is represented by $g_1$ and $g_2$. The Heaviside value, the symmetrical saturated function with respect, the sigmoid component, the Gaussian feature, the logistic sigmoid operation, and also the spline feature are some of the regularly utilized training algorithms that must be selected suitably for every layer [23]. The symmetrical saturated linear model was applied in both stages in this research. The training technique, which may be classified into two basic classes: supervised learning techniques and unsupervised training techniques, is among the most significant elements of an ANN. The Levenberg-Marquardt learning algorithm was utilized to optimize the FFNN emotional experiences in the developed learning approach, which was an offline required guidance. In an attempt to optimize ANN learning accuracy and generalization capacity, input samples were constructed using artificial information while following numerous principles.

To maintain adequate use across manufacturer's standards, the regulations used in the development of ANN for adjusting the power were predicated on the authorized rated capacity of the Li-ion battery [24]. To reduce Li-ion battery real situation and peaking currents, limits were set for the maximum batteries current flowing ($I_{\text{mc battery}}$) and maximum Li-ion battery discharging current ($I_{\text{md battery}}$). These restrictions were calculated as a fraction of the Li-ion batteries' maximum design power. To ensure the safety and quality of Li-ion batteries and increase their lifetime, a functional range of SOC was developed ($\text{SOC}_{\text{min battery}}$ and $\text{SOC}_{\text{max battery}}$). The SOC operating range for Lion packs is now to be set between 20% and 90%, which was defined as the optimal frequency. Due to the fundamental properties of SCs, there is no such limiting problem about the SOC operating range; thus, the established limits of $\text{SOC}_{\text{min SC}}$ and $\text{SOC}_{\text{max SC}}$ were set at 20% and 100%, accordingly.

Table 3: PV system values.

| | |
|---|---|
| Short-circuit power (A) ($I_{\text{SC}}$) | 4.96 A |
| Voltage coefficient of temperature ($\beta_{\text{OC}}$) | -150 mV/°C |
| Coefficients $Q_1$ | 0.01175 |
| Short-circuit temperature coefficient ($\alpha_{\text{SC}}$) | 3.00 mA/°C |
| Standard conditions of test ($T_{\text{STC}}$) | 25°C |

*3.5. Control System.* Closed-loop power converter and closed-loop voltage regulation are two types of techniques for the specified control strategy. Before turning on the machine, the operating settings were chosen [25]. A voltage regulation approach and three error signal processors with mechanisms are among the deployed control schemes (PI-awu). The power management approach among ESSs is executed with an FFNN which defines the current references ($I_{\text{ref bat}}$ and $I_{\text{ref sc}}$) in real-time information while taking into account the state of charge of a two parental, which is determined using the charge density method of counting, which quantifies this same charging/discharging current of such a battery/SC bundle and combines current over the period.

The result from $\text{PI}_{\text{ref}}$ a controller is another FFNN input. It works to eliminate the error signal between the reference voltage $I_{\text{ref bat}}$ and the DC bus voltage ($V_{\text{dc}}$) in the closed-loop voltage control scheme, and it functions to eliminate the error signal between the reference current ($I_{\text{dc bat}}$) and the load current in the closed-loop current control method $I_{\text{load}}$. The 2 different control systems ($\text{PI}_{\text{bat}}$ and $\text{PI}_{\text{SC}}$) perform by adapting the PWM duty cycle of such DC/DC adapters to calculate the output load of each inverter and remove the input signals in between time constants ($I_{\text{ref bat}}$ and $I_{\text{ref SC}}$) and the ESS current flow once currents ($I_{\text{ref bat}}$ and $I_{\text{ref SC}}$) have already been calculated through all the ANN.

*3.6. Algorithm of MPPT.* Thus, perturb and observe (P&O) technique was used to implement the MPPT algorithm, as shown in Figure 5. Low computing cost, simplicity of

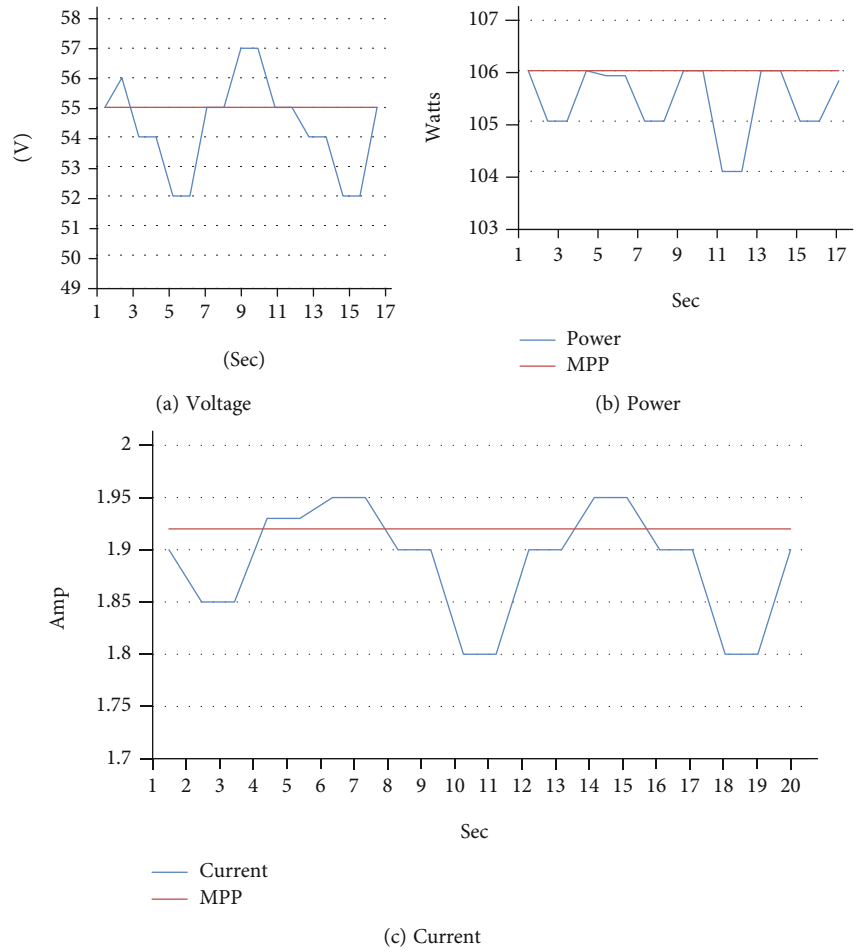


Figure 7: During all the system's operations, MPPT P&O algorithm signals were employed.

construction, and control are all characteristics of this approach [26]. It entails detecting the amount of electricity produced from the PV unit $(P_k)$ at a specific time $(t_k)$ and perturbing the DC/DC converter's PWM duty cycle $(\Delta d)$. The quantity of energy collected $(p_{k+1})$ is then evaluated at the instant $(t_{k+1})$ and contrasted to the level of voltage recovered at an instant $(t_k)$. If the perturbations lead to high voltage, the algorithms modify the converter's traditional operating frequency in the same manner as disturbance; otherwise, it alters the orientation of the disturbance. This is done until the peak power is attained.

*3.7. Optimization of PI Control.* Particle swarm optimization (PSO) was utilized with both control systems to identify the best settings of the PI controllers. The concepts of collaboration and behavior in society influenced the particle swarm algorithm. The method has a population of particles $(n_p)$, each of which symbolizes a potential response. The goal is to make the nanoparticles examine the multivariate state space $(d)$ to discover the best solution [27]. Equations (14) and (15) alter the speed $(v_i)$ and location $(x_i)$ from each $I$ particle in the populations $n_p$, respectively. The program analyzes each molecule's efficiency using a predetermined objective function (OF) and alters the speed of each particle $(v_i)$ as a result of three parts of equations at every iteration $t$. The photon's inertia (component of weight $w$) in retaining its current velocity is represented by the first component [28]. The second election adjusts each photon's efficiency towards its latest $(p_{\text{best}})$ so far, taking into consideration the cognitive variable $(s_1)$. Finally, the final term directs the electron to the greatest performance of the other particles in the group $(g_{\text{best}})$, while accounting for the social variable $(s_2)$. The results of optimizing the parameters connected with each controller are shown in Table 2.

$$v_{i,d}(t+1) = wv_{i,d}(t) + s_1 r_1 \left(p_{\text{best}\,i,d}(t) - x_{i,d}(t)\right) + s_2 r_2 \left(g_{\text{best}\,d} - x_{i,d}(t)\right), \tag{14}$$

$$x_{i,d}(t+1) = x_{i,d}(t) + v_{i,d}(t+1). \tag{15}$$

## 4. Result and Discussion

Modern computing analyses were carried to assess the performance of the system depicted in Figure 1. All equipment analyses were carried within standard conditions (irradiation of 1000 W/m$^2$ at 25°C) on an emulated PV with a PMPP of 106 Wp. The system's HESS was made up of 12 Li-ion battery

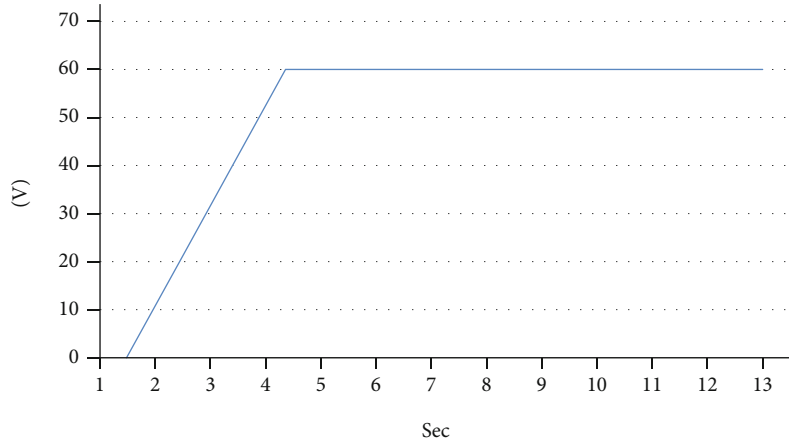


(a) The voltage at a constant state

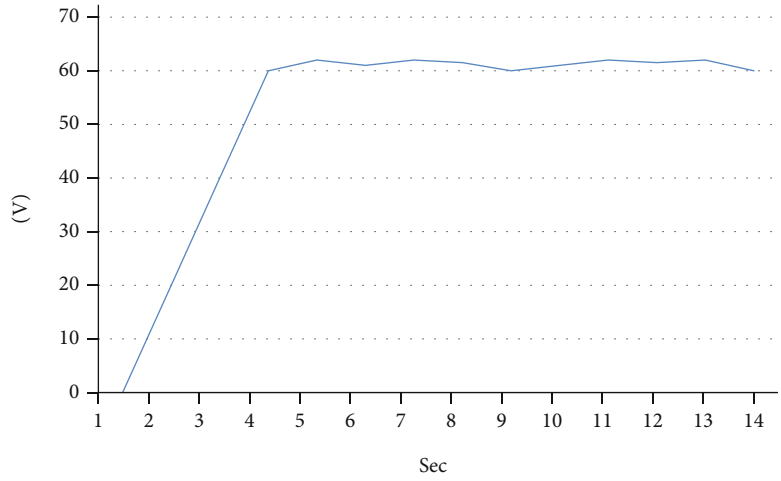


(b) The voltage at variable state

Figure 8: A voltage of DC bus.

cells that are connected and have a notional capacity of 2 Ah, as well as 12 SC cells in series connection and having a conventional capacitor of 500 F.

*4.1. Results of Photovoltaic Energy.* This employed a configurable source from Magna current, the DC SL 500-5.2, and its software configuration, solar photovoltaic curve emulation, to evaluate the MPPT algorithms for PV production. Figure 6 illustrates the *P-V* and *I-V* curves of the simulated PV, which are defined by $V_{oc} = 63$ V, $I_{SC} = 2$ A, $V_{MPP} = 55.53$ V, and $I_{MPP} = 1.911$ A, which equates to $P_{MPP} = 106$ Wp during standardized test circumstances ($1000\ W/m^2$ and 25°C). The values in Table 3 should be utilized in the mathematical modeling of a photovoltaic system.

The incredible system of PV is shown in Figure 7(b), with the MPP lines in orange. As can be seen, the energy collected from the PV is extremely near to the maximum power attainable in the PV throughout the test. This MPPT has a fast response time, only taking a few seconds to locate the MPP. This could attest to the outstanding results of the MPPT algorithm in use, and the DC/DC converters it is connected to. Figures 7(a) and 7(c) show the retrieved power of PV generation for the test. It could be observed that its MPPT P&O method implemented is just a basic, reliable, and efficient technique.

(a) Voltage
(b) Power
(c) Current

*4.2. Performance Test of HESS Control.* The testing used a voltage closed-loop control to simulate a realistic standalone operation. In this method, consistent power on the DC bus could be guaranteed throughout the system's operations. The test scenarios that were run concentrated on two parts of the power strategic approach that had been implemented: PV generation was less than the required load power ($P_{load} - P_{dc\,pv} < 0$); PV generation was higher than the required power system ($P_{load} - P_{dc\,pv} > 0$). As a result, it was feasible to evaluate the system's behavior whether the DC bus had an excess or deficiency of energy. Finally, two further situations were run to verify the state's opportunity to follow a control signal on the DC bus. During normal conditions, a DC bus voltage standard was implemented for the purpose, while in normal operation the system followed a dynamic DC bus voltage comparison. This research examines whether the system could

sustain a reference signal in the DC bus independent of PV generation power or the loads attached to that though.

Each ESS had a SOC of around 50% in the tests that were conducted. The maximum Li-ion battery charge/discharge mostly during realized testing was set to 0.4 A associated with system limits in terms of energy and to guarantee the program's stability.

The electricity taken from PV generation was larger than the requested load power in the first situation. As a result, excess HESS power would have to be assigned. However, because the current during the experiment surpassed the high voltage authorized for charging the Li-ion batteries, the surplus current had to be sent to the SCs, which assisted the Li-ion battery packs in accepting the additional current.

The power retrieved from PV generation would be less than the required peak load in the second example ($P_{\text{load}} - P_{\text{dc pv}} < 0$). As a result, the Li-ion batteries had to be discharged to supplement the PV generation and meet the load. However, the current required to fulfill the demand during testing surpassed the maximum current allowed for Li-ion battery degradation. As a result, the SCs had to be depleted in needed to aid PV generation the Li-ion battery in meeting the load demand.

The DC-link voltage even during an experiment using a closed-loop reference voltage is shown in Figure 8(a). All throughout the experiment, the DC-link voltage remained maintained at the predetermined value (60 V), demonstrating the energy management technique and controllers' high stability. The current development on the DC bus during perfect knowledge with changing power supply is shown in Figure 8(b). As can be observed, the system had a decent capability to follow a control voltage, indicating that the control method had a larger bandwidth.

(a) The voltage at a constant state

(b) The voltage at variable state

The results of the experimental testing confirmed the results of the earlier computational simulations, demonstrating the good response of the applied power management approach and the accompanying power management system. Scheme of control of the power management approach effectively demanded the SC within following circumstances, as in preceding computer analysis: (i) during the transient and steady-state responses and (ii) when the required power surpassed the Li-ion batteries' maximum output. As a result, the Li-ion batteries' dynamical load and peak market requirements were reduced, and their life was prolonged. Finally, the computational calculations and experimental setup demonstrated that the model battery management technique performs better.

## 5. Conclusion

The energy management controllers for a photovoltaic hybrid power system with such a power supply are presented in this research, which is developed on an artificial neural network. In hybrid renewable energy systems, the ANN controller may scale up enough energy and preserve sustainable management. This research proposes a unique HESS voltage regulation technique based on such an artificial neural network only intending to reduce Li-ion battery pressure in standalone renewables microgrids in switching device exchange situations. The suggested energy management method is capable of regulating the ESSs' flow of energy, controlling their charge or discharge power based on their SOC state and meeting the load requirements all across the system's operations. To demonstrate the practical information that can be extracted from a battery management technique, the provided system was constructed in hardware platforms, and realistic tests have been carried out. The conclusions back up the graph-theoretical experiments and ensure that the Li-ion cells are effectively protected as well as that the integrated controllers respond quickly. This shows that by implementing the proposed approach, the lifetime of Li-ion batteries could be extended.

## Data Availability

The data used to support the findings of this study are included within the article.

## Conflicts of Interest

The authors declare that there is no conflict of interest regarding the publication of this article.

## Acknowledgments

The authors would like to express their gratitude towards Saveetha School of Engineering, Saveetha Institute of Medical and Technical Sciences (formerly known as Saveetha University), for providing the necessary infrastructure to carry out this work successfully. This project was supported by Researchers Supporting Project number (RSP-2021/315), King Saud University, Riyadh, Saudi Arabia.

## References

[1] M. Boussetta, S. Motahhir, R. El Bachtiri, A. Allouhi, M. Khanfara, and Y. Chaibi, "Design and embedded implementation of a power management controller for wind-PV-diesel microgrid system," *International Journal of Photoenergy*, vol. 2019, 16 pages, 2019.

[2] A. Abusorrah, M. M. al-Hindawi, Y. al-Turki et al., "Stability of a boost converter fed from photovoltaic source," *Solar Energy*, vol. 98, pp. 458–471, 2013.

[3] P. Nirmala, G. Ramkumar, S. Sahoo et al., "Artificial intelligence to analyze the performance of the ceramic-coated diesel engine using digital filter optimization," *Advances in Materials Science and Engineering*, vol. 2021, Article ID 7663348, 10 pages, 2021.

[4] C. Ma, C. Li, X. Zhang, G. Li, and Y. Han, "Reconfiguration of distribution networks with distributed generation using a dual hybrid particle swarm optimization algorithm," *Mathematical Problems in Engineering*, vol. 2017, 10 pages, 2017.

[5] M. M. Rahman, M. Shakeri, S. K. Tiong et al., "Prospective methodologies in hybrid renewable energy systems for energy prediction using artificial neural networks," *Sustainability*, vol. 13, no. 4, p. 2393, 2021.

[6] J. A. Dhanraj, A. Mostafaeipour, K. Velmurugan et al., "An effective evaluation on fault detection in solar panels," *Energies*, vol. 14, no. 22, p. 7770, 2021.

[7] I. Aboudrar, S. El Hani, M. S. Heyine, and N. Naseri, "Dynamic modeling and robust control by ADRC of grid-connected hybrid PV-wind energy conversion system," *Mathematical Problems in Engineering*, vol. 2019, 19 pages, 2019.

[8] G. Ramkumar, S. Sahoo, T. M. Amirthalakshmi et al., "A short-term solar photovoltaic power optimized prediction interval model based on FOS-ELM algorithm," *International Journal of Photoenergy*, vol. 2021, Article ID 3981456, 2021.

[9] A. A. M. Nureddin, J. Rahebi, and A. Ab-BelKhair, "Power management controller for microgrid integration of hybrid PV/fuel cell system based on artificial deep neural network," *International Journal of Photoenergy*, vol. 2020, 21 pages, 2020.

[10] J. Faria, J. Pombo, M. Calado, and S. Mariano, "Power management control strategy based on artificial neural networks for standalone PV applications with a hybrid energy storage system," *Energies*, vol. 12, no. 5, p. 902, 2019.

[11] T. M. Amirthalakshmi, S. Ramesh, R. T. Prabu et al., "A novel approach in hybrid energy storage system for maximizing solar PV energy penetration in microgrid," *International Journal of Photoenergy*, vol. 2022, Article ID 3559837, 7 pages, 2021.

[12] X. Zhang, L. Liu, and Y. Dai, "Fuzzy state machine energy management strategy for hybrid electric UAVs with PV/fuel cell/battery power system," *International Journal of Aerospace Engineering*, vol. 2018, 16 pages, 2018.

[13] L. N. Khanh, J.-J. Seo, Y.-S. Kim, and D.-J. Won, "Power-management strategies for a grid-connected PV-FC hybrid system," *IEEE Transactions on Power Delivery*, vol. 25, no. 3, pp. 1874–1882, 2010.

[14] C. Pradhan, M. K. Senapati, S. G. Malla, P. K. Nayak, and T. Gjengedal, "Coordinated power management and control of standalone PV-hybrid system with modified IWO-based MPPT," *IEEE Systems Journal*, vol. 15, no. 3, pp. 3585–3596, 2021.

[15] S. Sukumar, M. Marsadek, A. Ramasamy, H. Mokhlis, and S. Mekhilef, "A fuzzy-based PI controller for power management of a grid-connected PV-SOFC hybrid system," *Energies*, vol. 10, no. 11, p. 1720, 2017.

[16] P. Sivasankari, S. Padmini, and R. C. Ilambirai, *Modelling control power management of grid connected hybrid PV battery diesel system*, *AIP Conference Proceedings 2112, 020103*, 2019.

[17] K.-M. Kang, B. Y. Choi, H. Lee et al., "Energy management method of hybrid AC/DC microgrid using artificial neural network," *Electronics*, vol. 10, no. 16, p. 1939, 2021.

[18] H. H. Ammar, A. T. Azar, R. Shalaby, and M. I. Mahmoud, "Metaheuristic optimization of fractional order incremental conductance (FO- INC) maximum power point tracking (MPPT)," *Complexity*, vol. 2019, 13 pages, 2019.

[19] O. O. Mengi and I. H. Altas, "A new energy management technique for PV/wind/grid renewable energy system," *International Journal of Photoenergy*, vol. 2015, 19 pages, 2015.

[20] V. Fulmali, S. Gupta, and M. F. Khan, "Modeling and simulation of boost converter for solar-PV energy system to enhance its output," in *2015 International Conference on Computer, Communication and Control (IC4)*, pp. 1–4, Indore, India, 2015.

[21] S. Kumaravel and S. Ashok, "Optimal power management controller for a stand-alone solar PV/wind/battery hybrid energy system," *Energy Sources, Part A: Recovery, Utilization, and Environmental Effects*, vol. 37, no. 4, pp. 407–415, 2015.

[22] S. Das and A. K. Akella, "A control strategy for power management of an isolated micro hydro-PV-battery hybrid energy system," in *2018 4th International Conference on Electrical Energy Systems (ICEES)*, pp. 397–401, Chennai, India, 2018.

[23] O. Charrouf, A. Betka, S. Abdeddaim, and A. Ghamri, "Artificial neural network power manager for hybrid PV-wind desalination system," *Mathematics and Computers in Simulation*, vol. 167, pp. 443–460, 2020.

[24] N. Mhusa, G. Nyakoe, and E. Mgaya, "Power management in photovoltaic-wind hybrid system based on artificial intelligence," *Journal of Multidisciplinary Engineering Science and Technology*, vol. 2, no. 1, 2015.

[25] S. Kumaravel and S. Ashok, *Adapted multilayer feedforward ANN based power management control of solar photovoltaic and wind integrated power system*, ISGT2011, India, 2011.

[26] M. Orabi, F. Hilmy, A. Shawky, J. A. A. Qahouq, E.-S. Hasaneen, and E. Gomaa, "On-chip integrated power management MPPT controller utilizing cell-level architecture for PV solar system," *Solar Energy*, vol. 117, pp. 10–28, 2015.

[27] V. Rashtchi, H. Kord, and A. Rohani, "Application of GA and PSO in optimal design of a hybrid photovoltaic/fuel cell energy system," *Fuel Cells*, vol. 3, p. 7, 2009.

[28] B. Benlahbib, N. Bouarroudj, S. Mekhilef et al., "Experimental investigation of power management and control of a PV/wind/fuel cell/battery hybrid energy system microgrid," *International Journal of Hydrogen Energy*, vol. 45, no. 53, pp. 29110–29122, 2020.